# Part I. Supplementary Figures

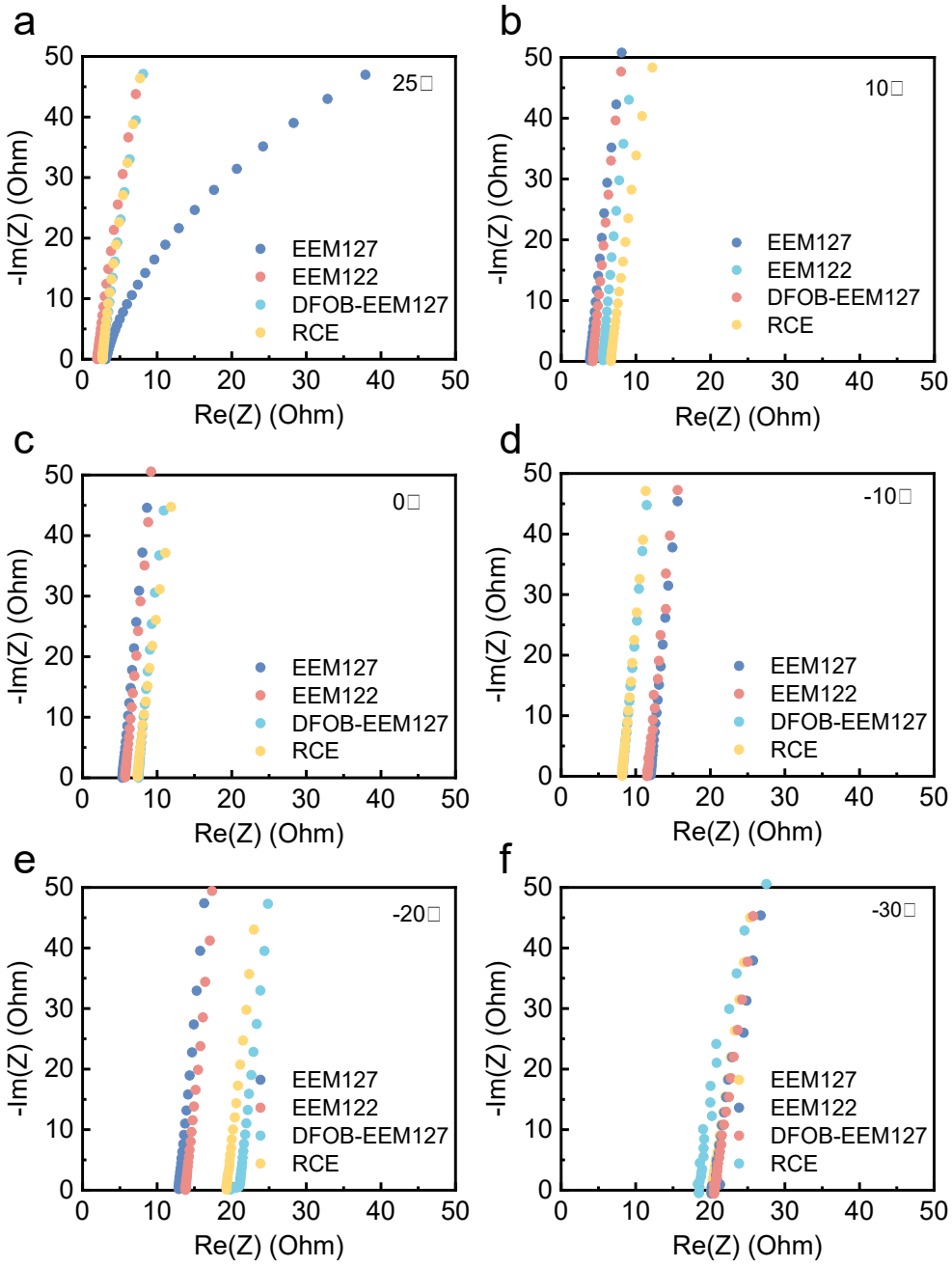


Fig. S1 Nyquist plots of four electrolytes at different temperatures. Two stainless-steel electrodes are used as blocking electrodes.

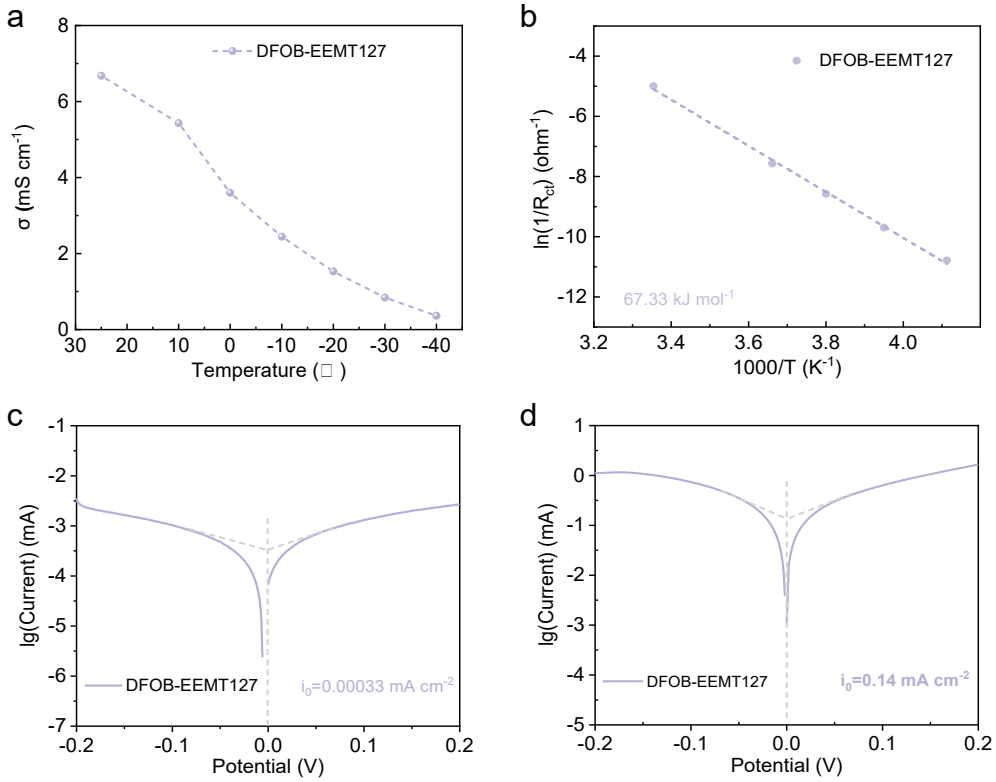


Fig. S2 The electrochemical properties of the DFOB-EEMT127(a) Ionic conductivity of different electrolytes in a wide temperature range. (b) The desolvation energies (Ea) of different electrolytes at low temperatures fitted by Arrhenius. Tafel curves of Li||Li symmetric cells in (c) -30℃, and (d) 25℃.

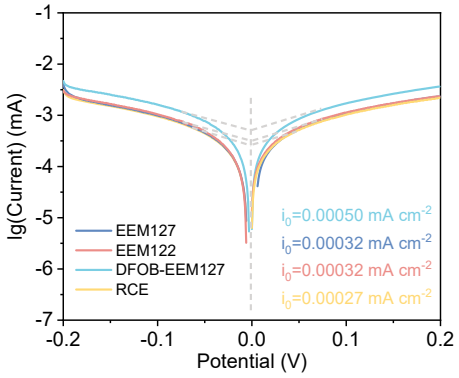


Fig. S3 Tafel curves of Li||Li symmetric cells with the prepared electrolytes in -30℃.

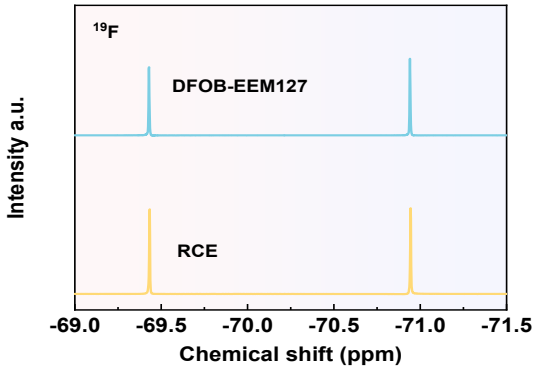


Fig. S4 $^{19}F$ NMR spectra of DFOB-EEM127 and RCE.

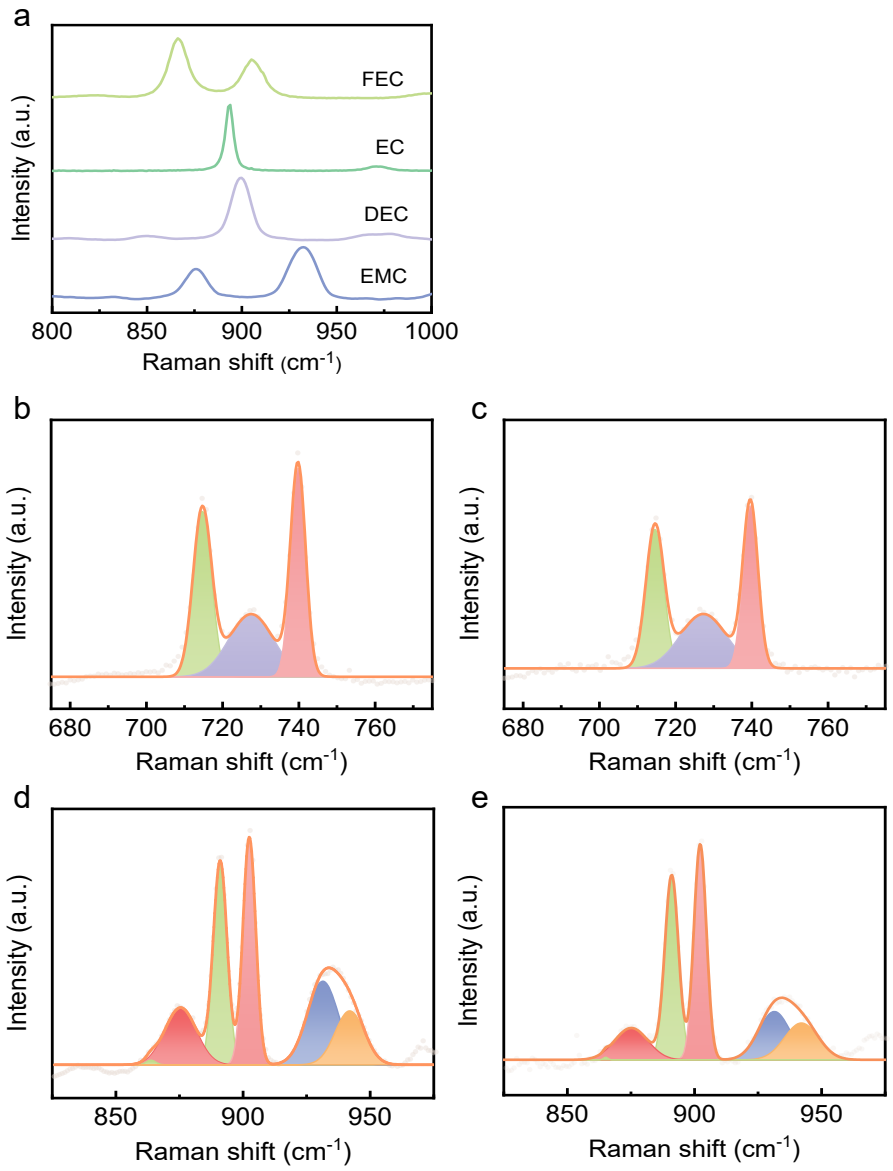


Fig. S5 (a) Raman spectra of different solvents. (b) EEM127 and (c) EEM122 in the Raman spectrum ranging from 675 $cm^{-1}$ to 775 $cm^{-1}$. (d) EEM127 and (e) EEM122 in the Raman spectrum ranging from 825 $cm^{-1}$ to 975 $cm^{-1}$.

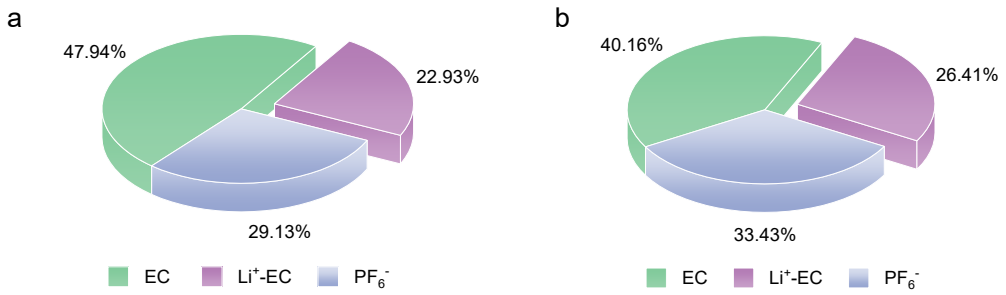


Fig. S6. The relative peak area ratios of the Raman spectra in the 675-775 $cm^{-1}$ range of (a) DFOB-EEM127 and (b) RCE.

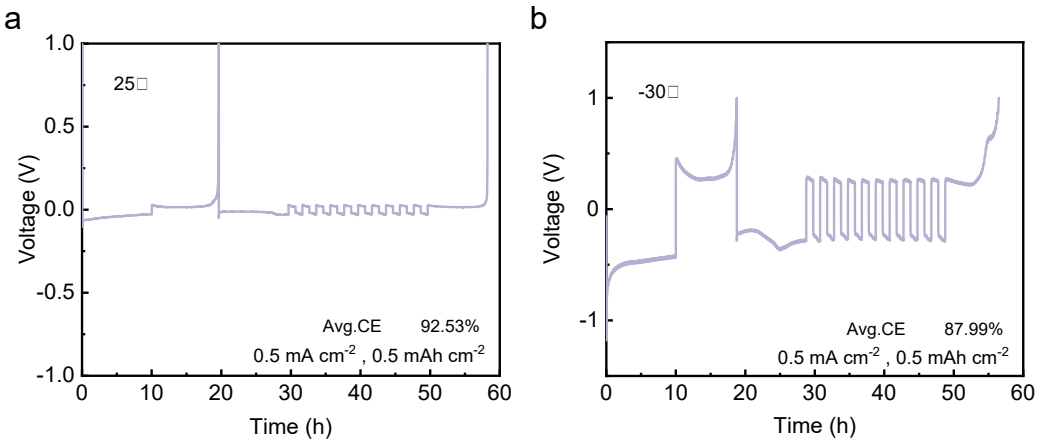


Fig. S7. Li plating/stripping CE evaluated by Li||Cu cells under (a) 25°C and (c) -30°C.

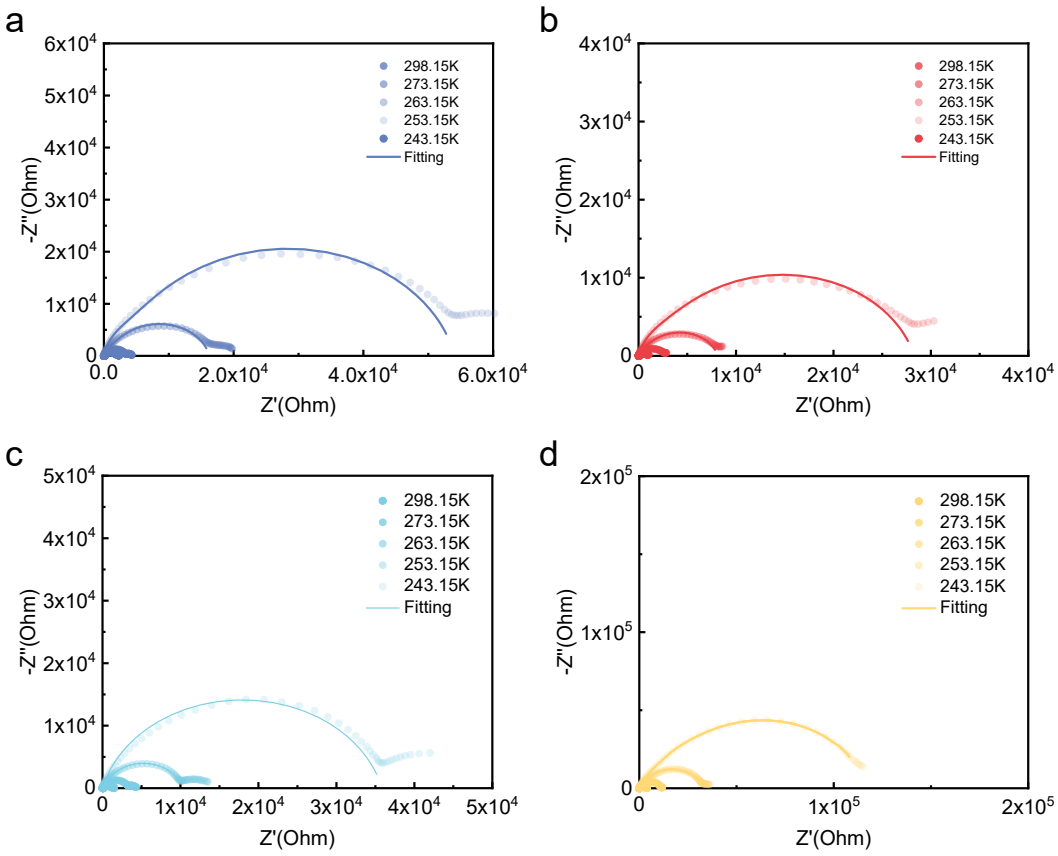


Fig. S8 (a) Nyquist plots of EEM122 at diffrent temperatures. (b) Nyquist plots of EEM127 at diffrent temperatures. (c) Nyquist plots of DFOB-EEM127 at diffrent temperatures. (d) Nyquist plots of RCE at diffrent temperatures.

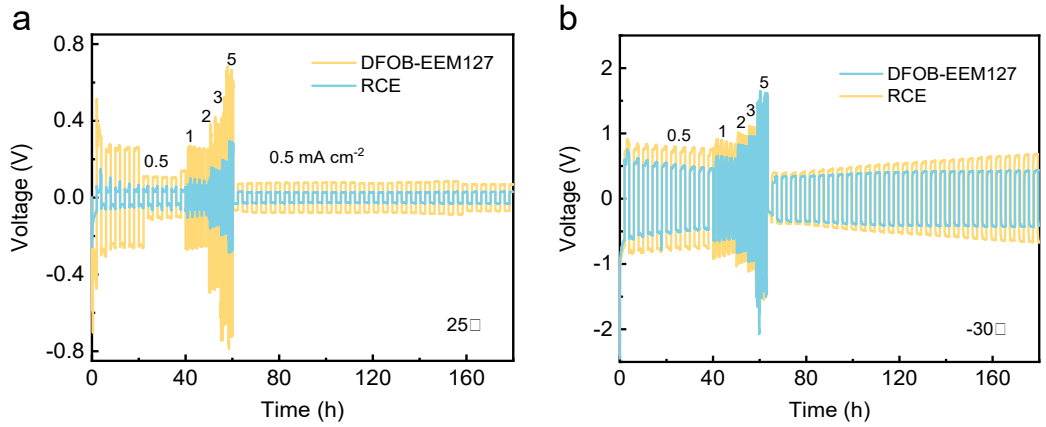


Fig. S9 Low-temperature rate performance of Li||Li symmetric cells at 0.5–5 mA $cm^{-2}$ and 0.5 mAh $cm^{-2}$

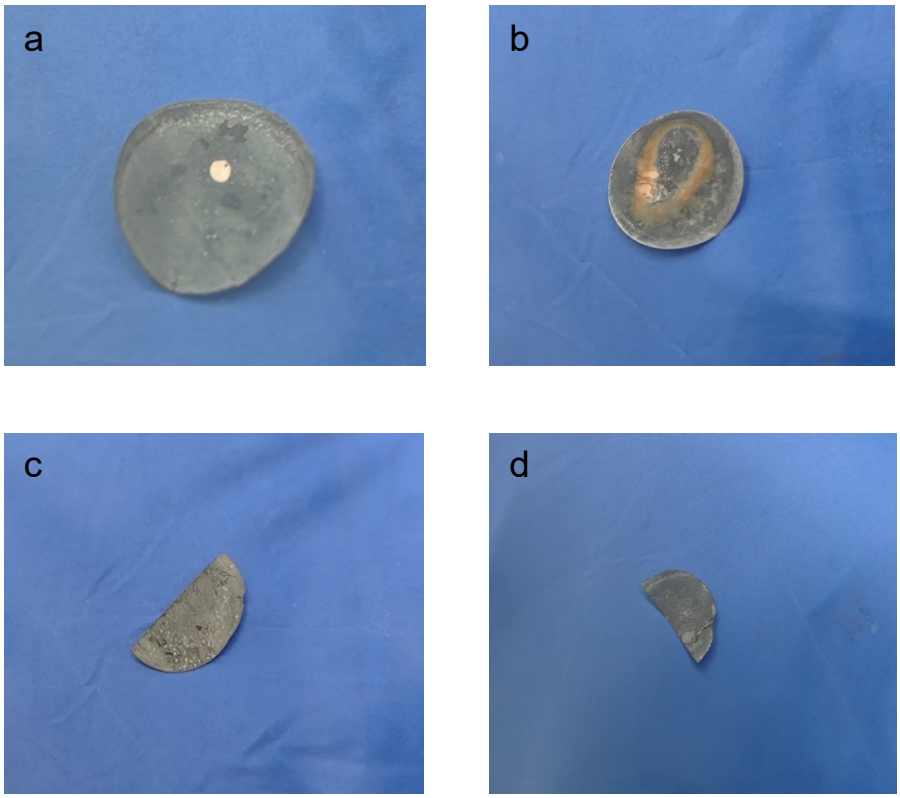


Fig. S10 (a) Top view of the Li deposition morphology in EEM127. (b) Top view of the Li deposition morphology in EEM122. (c) Top view of the Li deposition morphology in DFOB-EEM127. (d) Top view of the Li deposition morphology in RCE.

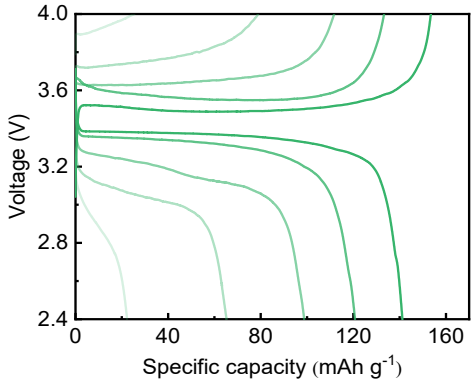


Fig. S11 Voltage profiles of a low-loading LFP||Li cell (1.7 mg $cm^{-2}$) measured at 0.1 C from 20 to -40°C.

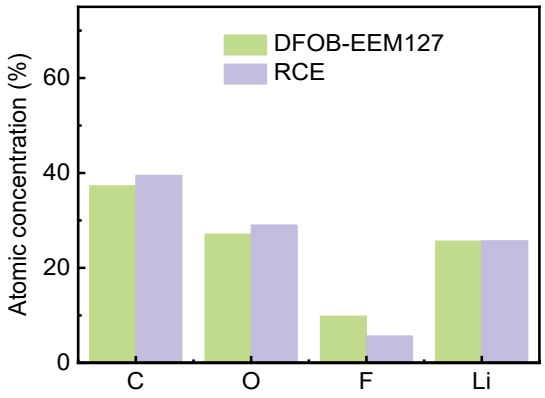


Fig. S12 Atomic concentration plots in DFOB-EEM127 and RCE.

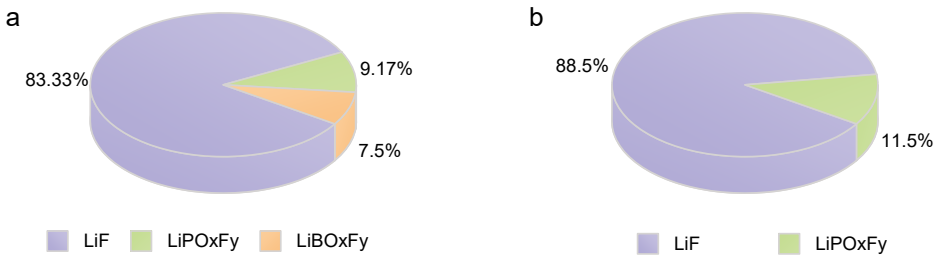


Fig. S13 The proportions of each component in the XPS F 1s.

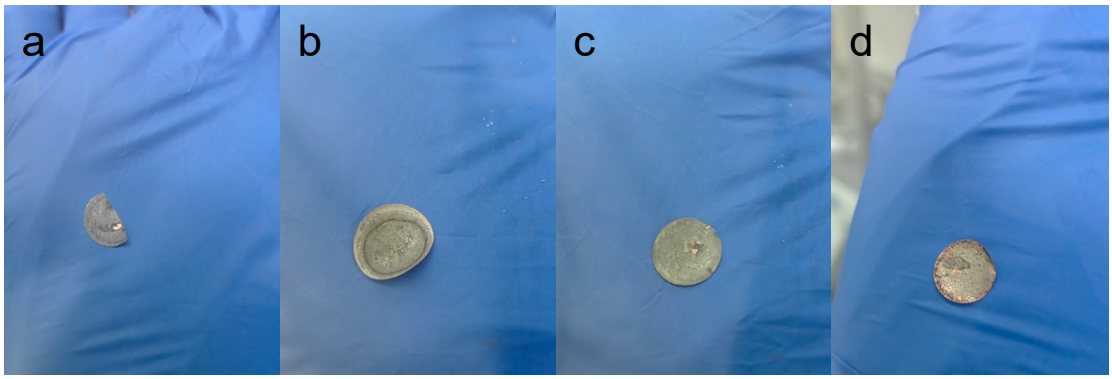


Fig. S14 (a) The images of the surface topography of the electrodes after cycling. in the EEM127. (b)The images of the surface topography of the electrodes after cycling. in the EEM122. (c) The images of the surface topography of the electrodes after cycling. in the EFOB-EEM127. (d) The images of the surface topography of the electrodes after cycling. in the RCE.

Table S1. The composition ratio of each electrolyte solution (w/w)

| Electrolytes | Mass fraction |
|---|---|
| EEM127 | $LiPF_6$: EC: EMC: FEC: TTE=13:27.5:56.5:0.5:2.5 |
| EEM122 | $LiPF_6$: EC: EMC: FEC: TTE=13:31.5:52.5:0.5:2.5 |
| DFOB-EEM127 | $LiPF_6$: LiDFOB: EC: EMC: FEC: TTE=10.5:2.5:27.5:56.5:0.5:2. |
| DFOB-EEMT127 | $LiPF_6$: LiDFOB: EC: EMC: FEC=10.5:2.5:27.5:56.5:0.5 |
| RCE | 1M $LiPF_6$-EC: DEC: DMC=1:1:1(v/v) |

Table S2. The physical and chemical properties of each solvent in the electrolyte solution

| | EC | FEC | DEC | EMC | DMC |
|---|---|---|---|---|---|
| Number of donors DN | 16.4 | 16 | 16 | 15.8-16 | 15.1 |
| Dielectric constant (F/m) | 89.8 | 85 | 2.8 | 2.9 | 3.1 |
| Melting point (℃) | 36.4 | 18 | -43 | -14 | 4.6 |
| Viscosity (mPa·s) | 1.93 | 1.5 | 0.75 | 0.65 | 0.59 |

Table S3. Ionic conductivity of different electrolytes in different temperatures.

| Electrolyte | 25℃ (mS $cm^{-1}$) | 10℃ (mS $cm^{-1}$) | 0℃ (mS $cm^{-1}$) | -10℃ (mS $cm^{-1}$) | -20℃ (mS $cm^{-1}$) | -30℃ (mS $cm^{-1}$) | -40℃ (mS $cm^{-1}$) |
|---|---|---|---|---|---|---|---|
| EEM127 | 6.318 | 4.312 | 3.331 | 2.436 | 1.742 | 1.102 | 0.45 |
| EEM122 | 6.945 | 3.813 | 3.010 | 2.239 | 1.547 | 0.961 | 0.45 |
| DFOB-EEM127 | 6.583 | 3.624 | 2.875 | 2.211 | 1.578 | 1.013 | 0.527 |
| RCE | 5.172 | 3.785 | 2.893 | 2.101 | 1.403 | 0.846 | 0.376 |